High Frequency Modeling of Granular Soft Magnetic Materials with Local Model Order Reduction

Antero Marjamäki, Rainer Schneckenleitner, Reda Elkhadrawy, and Paavo Rasilo

Electrical Engineering Unit, Tampere University, Tampere, Finland

A full-wave electromagnetic field equation in a cross section of a ferrite core, modeled as an array of grains, is solved with the finite element method utilizing local model order reduction techniques. With the traditional finite element method and a high number of grains, the resulting system becomes resource-intensive. The reduced approach greatly decreases the amount of degrees of freedom and the computational time for solving the resulting system.

Index Terms—**Domain decomposition, model order reduction, soft magnetic materials.**

I. INTRODUCTION

LOCAL model order reduction (LMOR) methods are methods which can be applied to eliminate excess amounts of degrees of freedom (DOFs) inside subregions of a domain [1], [2]. They can be applied to a wide range of problems such as eliminating the internal DOFs of windings in magnetoquasistatic problems [3]. The need for special techniques like LMOR typically arises when the problem has multi-scale features which, in traditional finite element (FE) approaches, will result in an extremely high number of DOFs. In this paper, we will use a randomized basis generation technique, which differs somewhat from the highly popular proper orthogonal decomposition (POD) technique which is used, e.g., in [4], [5].

Manganese-zinc ferrite cores are widely used in high-frequency power electronics applications because they offer low losses and high permeability at high frequency [6]. This kind of material can be modeled as a structure consisting of a large number of equivalent small sized grains separated by a thin boundary layer [7]. Modeling ferrite cores while considering such grain-scale structure is heavily expensive when standard FE solvers are used. Thus, fast and accurate solvers are needed to tackle such problems.

A popular way to tackle the multi-scale problem is homogenization [8]. Homogenization techniques assume that the field quantities inside a subdomain containing a micro-scale feature can be assumed homogeneous over the subdomain. It is however not always evident a priori when such an assumption is justifiable. Therefore homogenization is not applicable to all problems of this nature.

In this paper, a ferrite core is modeled while considering the grain-scale microstructure by taking a single grain which is modeled and meshed. Next a reduced order model of the grain is computed. The resulting grain model is then replicated and the grain domains are connected accordingly using Lagrange multipliers to form the grain structure. In this approach, the amount of DOFs is significantly reduced. Hence it can be used to fill the gap between homogenization methods and traditional FE analysis when homogenization may not be fully justified.
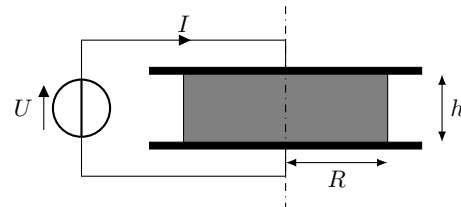
Fig. 1. An illustration of the impedance measurement and the dimensions of a disk-shaped ferrite core (gray area).

The novelty of this paper is to demonstrate the combination of the natural domain decomposition technique utilizing Lagrange multipliers, emerging from the ferrite's grain structure, in combination with LMOR techniques in order to speed up the simulation of granular magnetic materials. Furthermore, we demonstrate that the axisymmetric nature of the problem can be approximated as an affine dependency and hence the proposed ROM can be precomputed efficiently in the offline stage and then be used in the online stage with the optimal computational complexity [9].

II. COMPUTATIONAL MODELS

The problem under study is an impedance measurement of a disk-shaped ferrite sample, (see Fig. 1) with $h = 7.5\,\text{mm}$ and R varying based on the dimensions δ_g, δ_b (see. Fig. 3) and the number of individual grains in the array (see Fig. 2, left) denoted with G. The sample is placed between two conducting plates. A sinusoidal voltage is applied to the plates and the device determines the impedance of the sample based on the voltage, current and the phase difference between the two.

Frequency domain analysis and cylindrical coordinates r, φ and z are used. Considering the grain-scale microstructure of the core (see Fig. 2, right), the rectangular cross section in the r-z plane can be modeled as an array of square grains shown in Fig. 2, left. A 2-D axisymmetric FE model is constructed for solving the electromagnetic full-wave equation in the rectangular cross section of the core where $(r, z) \in [0, R] \times [0, \delta_\text{g} + 2\delta_\text{b}]$. The axisymmetric model is well justified due to the currents flowing through the sample in the r-z plane, from the top electrode to the bottom. The magnetic field is considered to have only a circumferential component:
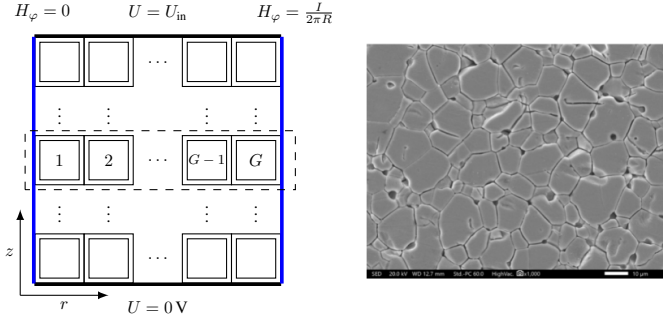
Fig. 2. Left: A grain array Ω_a with boundary conditions for H_φ. Because the same net current passes through each layer of grains in the z-direction, only one layer of grains is considered in the simulation. Right: a scanning electron microscope image of the ferrite material from [10].

$\mathbf{H} = H_\varphi(r, z)\mathbf{e}_\varphi$, where $\mathbf{e}_\varphi$ is the unit vector in the φ-direction. Furthermore, based on Ampère's law, we can conclude that the H_φ at $r = R$ does not depend on z for the whole outer edge of the sample. Therefore we can consider modeling only a single z-directional layer of the grain array and we can scale the results we obtain in the layer for the whole sample thickness h. The governing equations for the magnetic field strength $\mathbf{H}$ in a 2-D cross section of a disk core are

$$\nabla \times ((\sigma + j\omega\varepsilon)^{-1}\nabla \times \mathbf{H}) + j\omega\mu\mathbf{H} = 0 , \qquad (1)$$

$$H_\varphi(0, z) = 0 \qquad H_\varphi(R, z) = \frac{I}{2\pi R} . \qquad (2)$$

The impedance is calculated as

$$Z = \frac{\int_V \left((\sigma + j\omega\varepsilon)^{-1} \|\nabla \times \mathbf{H}\|^2 + j\omega\mu \|\mathbf{H}\|^2\right) dV}{|I|^2} , \quad (3)$$

where V is the sample disk volume, and $\|\cdot\|$ denotes the L_2-norm.

In the classical FE model, (1) is discretized with the Galerkin FEM with nodal elements for H_φ in the whole grain array. The weak form of the problem is

$$\int_{\Omega_a} \frac{1}{r}(\sigma + j\omega\varepsilon)^{-1}\nabla H_\varphi \cdot \nabla\phi \, dA$$
$$+ \int_{\Omega_a} \frac{1}{r} j\omega\mu H_\varphi\phi \, dA = 0 , \ \forall\phi \in \Phi(\Omega_a) \qquad (4)$$

in the whole grain array Ω_a (see Fig 2, left), where $\Phi(\Omega_a)$ denotes the set of test functions in Ω_a.

III. Local Model Order Reduction

In order to create the ROM for a grain, we consider only a single grain domain shown in Fig. 3. We use POD with an oversampling domain [2]. The ROM is parametrized with respect to the angular frequency ω. Because of the axisymmetry, each grain is located in different radial positions, and hence the effect of r is visible in the equations. The r dependency of the model is non-affine and it therefore needs to be approximated to obtain an affine decomposition, e.g., by using polynomials [9, p.194]. Here, a Taylor polynomial is
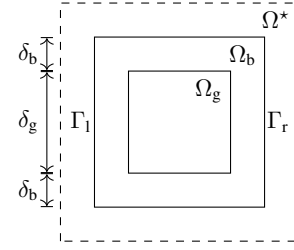

Fig. 3. The single grain cell. The grains are connected to each other through Γ_l and Γ_r. The oversampling domain $\Omega^\star$ is used only for the creation of the ROM.

used. The Taylor approximation for $1/r$ in the centerpoint r_i of the grain i is given by

$$\frac{1}{r} = \frac{1}{r_i} - \frac{1}{r_i^2}(r - r_i) + \frac{1}{r_i^3}(r - r_i)^2 + \dots . \qquad (5)$$

It turns out that in this case the zeroth order term is sufficient to produce well matching results. The zeroth order approximation means that the r-coordinate is actually considered as the constant $1/r_i$ in each grain. Using this approach, the approximated problem in a single grain i is expressed as

$$\frac{1}{r_i}\int_\Omega (\sigma + j\omega\varepsilon)^{-1}\nabla H_\varphi \cdot \nabla\phi \, dA$$
$$+ \frac{1}{r_i}\int_\Omega j\omega\mu H_\varphi\phi \, dA = 0 \ \ \forall\phi \in \Phi(\Omega) , \qquad (6)$$

where $\Omega = \Omega_b \cup \Omega_g$.

A. POD With an Oversampling Domain

In the reference grain cell we use an oversampling domain $\Omega^\star$ (see Fig. 3) to get a better reduction rate of the DOFs in the domain. The technique on obtaining the local reduced basis (RB) consists of setting randomized Dirichlet boundary conditions on the left and right sides of the grain. If the Dirichlet data is set directly to Γ_l and Γ_r, the resulting RB tends to have at least as many basis functions as there are DOFs on the boundary $\Gamma_l \cup \Gamma_r$. The purpose of $\Omega^\star$ is to let the randomized Dirichlet data to develop and smoothen out before entering the actual domain and hence the captured snapshots correspond to more naturally occuring exitations on the grain boundaries. This results in a more condensed RB. The reduction rate depends on the dimensions of the oversampling domain, which are chosen heuristically. A thicker oversampling layer results in less basis functions but increases the error. Typically the oversampling domain in FE-context is chosen to be in the order of a few layers of elements. The oversampling domain is considered to be vacuum.

The matrix form of (6) in $\Omega = \Omega_g \cup \Omega_b \cup \Omega^\star$ is

$$\frac{1}{r_i}\mathbf{S}^\star \mathbf{h}^\star = 0 . \qquad (7)$$

from which $1/r_i$ can be neglected, hence it will not affect the obtained reduced basis. Note that the matrix $\mathbf{S}^\star$ depends on the angular frequency ω. The equation can be split as

$$\begin{bmatrix} \mathbf{S}_{ii}^\star & \mathbf{S}_{il}^\star & \mathbf{S}_{ir}^\star \\ \mathbf{S}_{li}^\star & \mathbf{S}_{ll}^\star & 0 \\ \mathbf{S}_{ri}^\star & 0 & \mathbf{S}_{rr}^\star \end{bmatrix} \begin{bmatrix} \mathbf{h}_i^\star \\ \mathbf{h}_l^\star \\ \mathbf{h}_r^\star \end{bmatrix} = 0 . \qquad (8)$$

Next $\mathbf{h}_i^\star$ is solved in a single grain with different frequencies ω and random boundary values on $\Gamma_l^\star$ and $\Gamma_r^\star$ as

$$\mathbf{h}_i^\star = -\mathrm{S}_{ii}^{\star\,-1}\left(\mathrm{S}_{il}^\star \mathbf{h}_l^\star + \mathrm{S}_{ir}^\star \mathbf{h}_r^\star\right) \ . \tag{9}$$

From $\mathbf{h}_i^\star$ we extract only the values of DOFs inside $\Omega_b \cup \Omega_g$ and add them to the snapshot matrix X. The reduced basis U is then obtained by orthogonalizing X using a modified Gram-Schmidt algorithm introduced in [11]. Next, we check if the basis is good enough by computing the approximation error for a precomputed set of solutions H_{QA}, i.e.,

$$\left\|\mathbf{h}_p - \mathrm{U}\mathrm{U}^H\mathbf{h}_p\right\|_2 < \epsilon_{\mathrm{tol}} \ , \quad \forall\, \mathbf{h}_p \in H_{QA} \ . \tag{10}$$

The set H_{QA} is obtained by randomly choosing a set of samples of ω, $\mathbf{h}_l^\star$, $\mathbf{h}_r^\star$ and computing the corresponding solutions in $\Omega_b \cup \Omega_g$. Since the quality assurance samples are not the same as the snapshot samples, they offer an objective measure for the level of error of the ROM in each iteration. If condition (10) is false, we compute a new snapshot, add it to X, recompute the reduced basis U and recheck. When condition (10) is met, we consider the reduced basis ready.

This approach differs from the usual way the POD basis is computed, which uses the singular value decomposition (SVD). After sampling the parameters and computing the snapshots, SVD is applied and only the significant singular vectors are chosen into the reduced basis. In SVD based approaches, one needs to have a set of snapshots computed completely before generating the reduced basis. If new snapshots are added, one needs to recompute the basis for the whole snapshot set. This is computationally expensive especially when there are multiple parameters to be sampled.

In the approach presented in this paper, we extend the basis gradually until it is good enough. Therefore we do not need any a priori information on the location or amount of the snapshot parameters. The randomized approach is best suited when the ROM has many parameters or the associated high-fidelity FE problem is very time-consuming to solve.

B. Assembling the Reduced System

To utilize the affine decomposition in the grain array level we introduce matrices K and T as

$$[\mathrm{K}]_{kl} = \int_\Omega (\sigma + j\omega\varepsilon)^{-1}\nabla\phi_k \cdot \nabla\phi_l \,\mathrm{d}A \ , \tag{11}$$

$$[\mathrm{T}]_{kl} = \int_\Omega \mu\, \phi_k\, \phi_l \,\mathrm{d}A \ , \tag{12}$$

where $\phi_k \in \Phi(\Omega)$ and $\phi_l \in \Phi(\Omega)$ are FE trial and test functions, respectively. Next, we introduce the reduced matrices

$$\tilde{\mathrm{K}} = \mathrm{U}^H\mathrm{K}\mathrm{U} \ , \quad \tilde{\mathrm{T}} = \mathrm{U}^H\mathrm{T}\mathrm{U} \ . \tag{13}$$

The matrices $\tilde{\mathrm{K}}$ and $\tilde{\mathrm{T}}$ are reused for all different frequencies. The resulting frequency dependent reduced system matrix in grain i can now be computed as

$$\tilde{\mathrm{S}}_i = \frac{1}{r_i}\left(\tilde{\mathrm{K}} + j\omega\tilde{\mathrm{T}}\right) \ . \tag{14}$$

Next a block-diagonal matrix $\tilde{\mathrm{S}} = \mathrm{diag}\left(\tilde{\mathrm{S}}_1, \cdots, \tilde{\mathrm{S}}_G\right)$ is defined. The matrices R_r and R_l pick the entries of the DOF vector of the internal regions of $\Omega_b \cup \Omega_g$ corresponding to Γ_r and Γ_l respectively. We denote the matrix which maps the values of the DOFs in Γ_r to Γ_l as D_{lr}. This matrix is used to ensure the continuity of the field between grains. The meshes of Γ_l and Γ_r are made conforming.

The total reduced system is then

$$\begin{bmatrix} \tilde{\mathrm{S}} & \tilde{\mathrm{B}}^H \\ \tilde{\mathrm{B}} & \end{bmatrix}\begin{bmatrix} \tilde{\mathbf{x}} \\ \boldsymbol{\lambda} \end{bmatrix} = \begin{bmatrix} \\ \mathbf{F} \end{bmatrix} \ , \tag{15}$$

where

$$\tilde{\mathrm{B}} = \begin{bmatrix} \mathrm{D}_{lr}\mathrm{R}_r\mathrm{U} & \mathrm{R}_l\mathrm{U} & & \\ & & \ddots & \\ & & \mathrm{D}_{lr}\mathrm{R}_r\mathrm{U} & \mathrm{R}_l\mathrm{U} \\ \mathrm{R}_l\mathrm{U} & & & \\ & & & \mathrm{R}_r\mathrm{U} \end{bmatrix} \tag{16}$$

consists of the couplings between the grains and equations to set the boundary conditions, $\tilde{\mathbf{x}}^T = \begin{bmatrix} \tilde{\mathbf{h}}_1^T & \cdots & \tilde{\mathbf{h}}_G^T \end{bmatrix}$, and $\boldsymbol{\lambda}^T = \begin{bmatrix} \boldsymbol{\lambda}_1^T & \cdots & \boldsymbol{\lambda}_G^T & \boldsymbol{\lambda}_0^T & \boldsymbol{\lambda}_R^T \end{bmatrix}^T$, where $\boldsymbol{\lambda}_0$ and $\boldsymbol{\lambda}_R$ are the Lagrange multipliers used to set the boundary conditions on the left boundary of the first grain, and the right boundary of the last grain, respectively. The blocks consisting of zeros are left empty for clarity. The vector $\mathbf{F} = \begin{bmatrix} \cdots & \mathbf{F}_0^T & \mathbf{F}_R^T \end{bmatrix}^T$ consists of the aforementioned boundary values. Matrices $\tilde{\mathrm{K}}, \tilde{\mathrm{T}}$, and $\tilde{\mathrm{B}}$ can all be precomputed in the offline phase, and they are reused for different frequencies in the impedance computation.

A high-fidelity model and the ROM were implemented in Python utilizing GMSH's Python API [12]. To solve the resulting equation systems, both models are using SuperLU through the SciPy library.

IV. RESULTS AND DISCUSSION

The ROM was verified against traditional FE simulations. The grain dimensions and material parameters are shown in Table I. The properties of the ROM obtained for the grain are presented in Table II. The performance was compared in four cases with 100, 200, 1000, and 2200 grains. All computations were run in a Lenovo ThinkPad T14 with an i7-1165G7 CPU and 32GB of RAM. The simulated impedance can be seen in Fig. 4 left. Fig. 4 right shows the error in a single grain in the grain array with respect to it's r-position. As expected the highest error, $2.54\,\%$, is near the symmetry axis. Fig. 5 shows field plots of the magnitudes of H_φ and it's curl $\nabla \times \mathbf{H} = \mathbf{J} + \frac{\partial \mathbf{D}}{\partial t}$. At $1\,\mathrm{MHz}$ there is a resonance effect happening, which can be seen in the distribution of the magnetic field.

To analyze the reduction of computational resources, let us first analyze the number of DOFs in the ROM and the high-fidelity model. Let M denote the number of DOFs in a single grain, M_b denote the number of DOFs on $\Gamma_l \cup \Gamma_r$, and N denote the number of DOFs in the ROM of the grain. The full FE-model would contain $(M - M_b)G + M_b$ DOFs. The ROM contains $NG + (G-1)M_b + 2M_b$ DOFs. The numbers of DOFs for the three considered cases are presented in Table III. The single grain problem was reduced approximately by a factor of five, but the full grain array problem only by approximately the factor of three. This is because the full system includes also the Lagrange multipliers needed to couple the grains together.

TABLE I
DIMENSIONS AND MATERIAL PARAMETERS OF THE GRAINS.

parameter	value	parameter	value
$\delta_{\mathrm{g}}(\mu m)$	11.0	μ_{g}	$(2100 + 0.20j)\mu_0$
$\delta_{\mathrm{b}}(nm)$	68.4	μ_{b}	$(1.00 + 17.8j)\mu_0$
$\sigma_{\mathrm{g}}(\mathrm{S})$	28.7	ε_{g}	$(1.40 + 3.50j)\varepsilon_0$
$\sigma_{\mathrm{b}}(\mu\mathrm{S})$	15.0	ε_{b}	$(21.5 + 4.40j)\varepsilon_0$

TABLE II
PROPERTIES OF THE REDUCED ORDER MODEL FOR THE GRAIN.

ROM property	value
DOFs per grain	81
Reduced DOFs per grain	14
size reduction (%)	82.7
ROM offline (sec)	0.31

The frequency range of the simulations was $1\,\mathrm{kHz} - 10\,\mathrm{MHz}$ from which we sampled 84 frequencies. A ROM valid for a larger frequency range requires more snapshots and therefore produces a larger reduced basis for the ROM. Also, utilizing the affine decomposition for additional parametric dependencies, e.g., σ_{g}, σ_{b}, ε_{g}, ε_{b}, μ_{g}, μ_{b} will increase the dimension of the reduced basis further.

The computational times in Table II and Table III exclude the meshing times which grow larger for grain arrays with a high number of grains. In the ROM it is only required to mesh one grain, including the oversampling domain.

Table III shows the computed relative root-mean square error (RRMSE) of the impedance given by the full FE and reduced FE models for the four different cases. The accuracy of the obtained ROM is high, but reducing the number of basis functions further from 14, in order to, e.g., trade accuracy for speed, causes a complete breakdown of the model.

V. CONCLUSION

A randomized LMOR technique was applied to model a ferrite disk using an axisymmetric 2-D model consisting
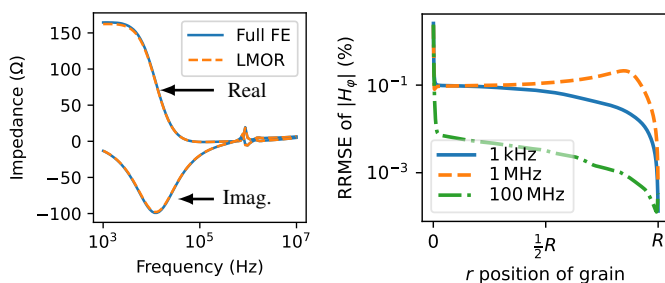
Fig. 4. Left: impedance computed with a full FE model and the LMOR model. Right: the RRMSE of $|H_\varphi|$ w.r.t the position of the grain when $G = 1000$.

TABLE III
THE NUMBERS OF DOFS BETWEEN THE HIGH-FIDELITY MODEL AND THE ROM WITH DIFFERENT NUMBER OF GRAINS IN THE ARRAY.

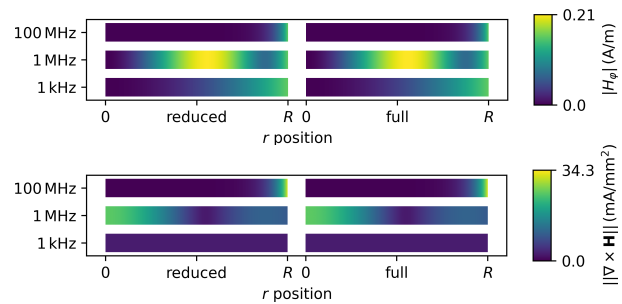| G	100	200	1000	2200
ROM DOFs total	2309	4609	23009	52809
full DOFs total	7209	14409	72009	158409
size reduction (%)	68.0	68.0	68.0	68.0
ROM online (sec)	0.48	0.94	8.43	14.3
ROM total (sec)	0.79	1.25	8.74	14.6
full total (sec)	1.44	4.21	19.57	38.0
RRMSE (%)	0.01	0.02	0.15	0.57

Fig. 5. The field plots of $|H_\varphi|$ and $||\nabla \times \mathbf{H}||$ in the ferrite disk using the reduced and full models in the $G = 1000$ case.

of simplified ferrite grains. The LMOR technique reduces the number of DOFs and speeds up the computation of the impedance of the sample for a frequency sweep. The technique seems promising whenever there is a naturally emerging way to split the problem domain into repeating subdomains. It may be useful to speed up parameter optimization or the forward problem of an inverse problem where repeated solving of the system with varying parameters is required.

ACKNOWLEDGMENTS

REFERENCES

[1] K. Smetana, and A. T. Patera, "Optimal Local Approximation Spaces for Component-Based Static Condensation Procedures," *SIAM J. Sci. Comput.,* vol. 38, no. 5, pp. 3318–3356, 2016.

[2] A. Buhr, and K. Smetana, "Randomized Local Model Order Reduction," *SIAM J. Sci. Comput.*, vol. 40, no. 4, pp. A2120–A2151, 2018.

[3] D. Schmidthäusler, S. Schöps and M. Clemens, "Reduction of Linear Subdomains for Non-Linear Electro-Quasistatic Field Simulations," *IEEE Trans. Magn.,* vol. 49, no. 5, pp. 1669–1672, 2013.

[4] Y. Paquay, C. Geuzaine, R. Hasan and R. V. Sabariego, "Reduced-Order Model Accounting for High-Frequency Effects in Power Electronic Components," *IEEE Trans. Magn.,* vol. 52, no. 3, pp. 1–4, 2016.

[5] L. Montier, T. Henneron, S. Clénet and B. Goursaud, "Model Order Reduction Applied to a Linear Finite Element Model of a Squirrel Cage Induction Machine Based on POD Approach," *IEEE Trans. Magn.,* vol. 57, no. 6, pp. 1–4, 2021.

[6] S. Lin, et al., "Review of dimensional resonance effect for high frequency magnetic components," *in Proc. EPE'19 ECCE,* Genova, Italy, 2019.

[7] F. Fiorillo, et al., "Eddy-Current Losses in Mn-Zn Ferrites," *IEEE Trans. Magn.,* vol. 50, no. 1, pp. 1–9, 2014.

[8] O. Bottauscio, M. Chiampi, A. Manzi, "Multiscale modeling of heterogeneous magnetic materials," *Int. J. Numer. Model.*, vol. 27, no. 3, pp. 373–384, 2014.

[9] A. Quarteroni, A. Manzoni and F. Negri "Reduced Basis Methods for Partial Differential Equations," *Springer Cham.*, Switzerland, 2016.

[10] R. Elkhadrawy, J. Ruuskanen, V. Tsakaloudi, K. Lahti and P. Rasilo, "2-D FEM-Based Approach for Identifying Intrinsic Material Parameters of Mn-Zn Ferrite Cores," in Proc. CEFC, Denver, CO, USA, 2022, pp. 1–2.

[11] A. Buhr, C. Engwer, M. Ohlberger and S. Rave, "A numerically stable a posteriori error estimator for reduced basis approximations of elliptic equations," ArXiv, 2014, available (accessed 18.04.2023) https://arxiv.org/pdf/1407.8005.pdf.

[12] C. Geuzaine and J.-F. Remacle, "Gmsh: a three-dimensional finite element mesh generator with built-in pre- and post-processing facilities," *Int. J. Numer. Methods Eng.*, vol. 79, no. 11, pp. 1309–1331, 2009.